Electronic Supplementary Information

Emission wavelength dependence on rISC rate in TADF compounds with large conformational disorder

Tomas Serevičius,*[a] Rokas Skaisgiris,[a] Jelena Dodonova,[b] Laimis Jagintavičius,[b] Jonas Bucevičius,[b] Karolis Kazlauskas, [a] Saulius Juršėnas[a] and Sigitas Tumkevičius[b]

[a]*Institute of Photonics and Nanotechnology, Faculty of Physics, Vilnius University, Sauletekio 3, LT-10257 Vilnius, Lithuania*

[b]*Institute of Chemistry, Faculty of Chemistry and Geosciences, Vilnius University, Sauletekio 3, LT-10257, Vilnius, Lithuania*

**Corresponding author: tomas.serevicius@tmi.vu.lt*

Table of Contents

Experimental

Reagents and solvents were purchased directly from commercial suppliers; solvents were purified by known procedures. Thin layer chromatography was performed using TLC-aluminum sheets with silica gel (Merck 60 F254). Visualization was accomplished by UV light. Column chromatography was performed using Silica gel 60 (0.040-0.063 mm) (Merck). NMR spectra were recorded on a Bruker Ascend 400 (400 MHz and 100 MHz for ^{1}H and ^{13}C, respectively). ^{1}H NMR and ^{13}C NMR spectra were referenced to residual solvent peaks. Melting points were determined in open capillaries with a digital melting point IA9100 series apparatus (ThermoFischer Scientific) and were not corrected. High Resolution Mass Spectrometry (HRMS) analyses were carried out on a quadrupole, time-of-flight mass spectrometer (microTOF-Q II, Bruker) or on a Dual-ESI Q-TOF 6520 (Agilent Technologies) mass spectrometer. Cyclic voltammetry experiments were performed on the Edaq ER466 Integrated Potentiostat System. Pt/Ti wire, glassy carbon disk [Ø 3.0 mm] and Ag/AgCl were used as counter, working, and reference electrodes, respectively. In all cases, CV experiments were performed in DMF (*N*,*N* – dimethylformamide) with tetrabutylammonium perchlorate - as supporting electrolyte (0.1 M) under N_2 flow; concentrations of compounds were 0.002 M. The scan rate was 50 mV s^{-1}. Absorption and emission spectra of pyrimidine derivatives were assessed in dilute 10^{-5} M toluene solutions and 1 wt% PMMA films. PMMA films of phenothiazine-pyrimidine derivatives were prepared by dissolving each material and PMMA at appropriate ratios in toluene solutions and then wet-casting the solutions on quartz substrates. Absorption spectra were recorded by UV-Vis-NIR spectrophotometer Lambda 950 (Perkin Elmer). Time-integrated fluorescence spectra, time-resolved fluorescence spectra, phosphorescence spectra and fluorescence decay transients were measured using nanosecond YAG:Nd^{3+} laser NT 242 (Ekspla, τ = 7 ns, pulse energy ~200 μJ, λ_{ex}=300 – 460 nm, repetition rate 10 Hz) and time-gated iCCD camera New iStar DH340T (Andor). Time-integrated fluorescence spectra were obtained using integration time larger than TADF lifetime. Fluorescence transients were obtained by exponentially increasing delay and integration time. This allows to record up to 10 orders of magnitude in time and intensity of the fluorescence decay[1]. Toluene solutions were degassed by using freeze-pump-thaw method. Polymer samples were mounted in closed cycle He cryostat (Cryo Industries 204N) for measurements in both oxygen-saturated and oxygen-free conditions. Temperature dependent measurements were performed in the same closed cycle He cryostat (Cryo Industries 204N).

Quantum chemical calculations of ground-state geometries, electronic excitation energies, oscillator strengths of the singlet and triplet transitions, spatial distributions of electron density for frontier orbitals were performed by using density functional theory (DFT) as implemented in the Gaussian 09 software package at the B3LYP/6-31G(d) level[2]. Polarizable Continuum Model (PCM) was used to estimate the solvation behaviour of toluene surrounding.

Synthesis

a) 10-(4-Bromo-3-methylphenyl)-10H-phenothiazine (I)

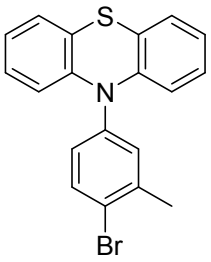

Phenothiazine (200 mg, 1 mmol), $Pd(OAc)_2$ (11.2 mg, 0.05 mmol, 5 mol %), PCy_3*HBF_4 (36.9 mg, 0.1 mmol, 10 mol %), 1-bromo-4-iodo-2-methylbenzene (360 mg, 1.2 mmol), NaO*t*-Bu (289 mg, 3 mmol) and toluene (4 mL) were placed in a screw-cap vial equipped with a magnetic stir bar. The vial was purged with argon and the reaction mixture was stirred vigorously at 110 °C for 24 h under argon atmosphere. After completion of the reaction, water (25 mL) was added and the aqueous solution was extracted with chloroform (4×25 mL). The combined extract was dried with anhydrous Na_2SO_4, filtered and chloroform was removed by distillation under reduced pressure. Residue was purified by column chromatography using chloroform:petroleum ether (1:9) as an eluent to give compound **I** as a yellow solid (288 mg, 78%), mp 146 °C. ^{1}H NMR (400 MHz, $CDCl_3$) δ (ppm): 7.79 (1H, d, *J* = 8.3 Hz, Ph-5-H); 7.32 (1H, d, *J* = 2.3 Hz, Ph-2-H); 7.14 (1H, dd, *J* = 8.3 Hz, *J* = 2.3 Hz, Ph-6-H); 7.08 (2H, dd, *J* = 7.6 Hz, *J* = 1.7 Hz, phenothiazine-4,6-H); 6.85–6.95 (4H, m, phenothiazine-2,3,7,8-H); 6.29 (2H, d, *J* = 7.6 Hz, phenothiazine-1,9-H); 2.51 (3H, s, CH_3). ^{13}C NMR (100 MHz, $CDCl_3$) δ (ppm): 143.9, 141.0, 140.3, 134.5, 132.7, 129.6, 126.94, 126.90, 124.3, 122.8, 120.7, 116.3, 23.2.

General procedure for the synthesis of boronic acids. To a solution of 10-(4-bromo-3-methylphenyl)-10*H*-phenothiazine (1.29 g, 3.5 mmol) or 1,4-dibromo-2,5-dimethylbenzene (0.92 g, 3.5 mmol) in 50 mL of anhydrous tetrahydrofuran 2.5 M *n*-butyllithium solution in hexanes (2.1 mL, 5.25 mmol) was added dropwise at −78 °C under argon atmosphere and vigorous stirring. After stirring for 1 h, trimethyl borate (1.2 mL, 10.5 mmol) was added at the same temperature and allowed to warm to room temperature overnight under stirring. Then 1 M hydrochloric acid was added dropwise until an acidic solution was obtained. After stirring for 1 h, the reaction mixture was poured into water and extracted with chloroform (4×20 mL). The combined organic layer was dried over anhydrous Na_2SO_4, filtered and evaporated to dryness. The crude product was then purified by precipitating with petroleum ether to afford the desired boronic acid.

b) 2-Methyl-4-(10*H*-phenothiazin-10-yl)phenylboronic acid (2).

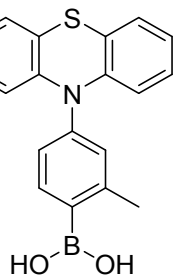

Light brown solid (0.816 g, 70%), mp 179-180 °C. ^{1}H NMR (400 MHz, DMSO-d_6) δ (ppm): 7.70 (1H, d, *J* = 8 Hz, Ph-6-H); 7.16-7.18 (2H, m, Ph-3,5-H); 7.07 (2H, d, *J* = 8 Hz, phenothiazine-4,6-H); 6.84-6.96 (4H, m, phenothiazine-2,3,7,8-H); 6.22 (2H, d, *J* = 8 Hz, phenothiazine-1,9-H); 2.48 (3H, s, CH_3). ^{13}C NMR (100 MHz, DMSO-d_6) δ (ppm): 144.9, 144.0, 141.1, 135.9, 130.8, 127.72, 127.68, 127.1, 126.5, 123.1, 119.9, 116.6, 22.50.

c) 4-Bromo-2,5-dimethylphenylboronic acid (3)

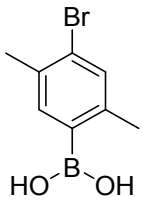

White solid (0.32 g, 40%), mp 228-230 °C. ^{1}H NMR (400 MHz, DMSO-d6) δ (ppm): 7.76 (1H, s, C-6-H); 7.36 (1H, s, C-3-H); 2.58 (3H, s, CH_3); 2.32 (3H, s, CH_3). ^{13}C NMR (100 MHz, DMSO-d^6) δ (ppm): 143.5, 137.7, 133.5, 133.2, 125.8, 117.5, 22.5, 21.7.
NMR spectra of compound **3** match with those described in ref. [3].

General procedure for the synthesis of PTZ-mPYR and PTZ-mPYRCl. 4,6-Dichloropyrimidine (**1a**) (50 mg, 0.336 mmol) or 2,4,6-trichloropyrimidine (**1b**) (61.6 mg, 0.336 mmol), $Pd(OAc)_2$ (7.5 mg, 0.034 mmol, 10 mol %), PPh_3 (17.6 mg, 0.067 mmol, 20 mol %), corresponding boronic acid (0.829 mmol, 2.5 equiv.) and aqueous Na_2CO_3 (221 mg, 2.08 mmol) and glyme (3 mL) were placed in a screw-cap vial equipped with a magnetic stir bar. The reaction mixture was stirred vigorously at 90 °C for 24 h under argon atmosphere. After completion of the reaction, water (20 mL) was added and the aqueous solution was extracted with chloroform (4×20 mL). The combined extract was dried with anhydrous Na_2SO_4, filtered and chloroform was removed by distillation under reduced pressure. Residue was purified by column chromatography using chloroform:petroleum ether (1:2) as eluent to give the corresponding **PTZ-mPYR** and **PTZ-mPYRCl**.

d) 4,6-Bis(2-methyl-4-(10*H*-phenothiazin-10-yl)phenyl)pyrimidine (PTZ-mPYR)

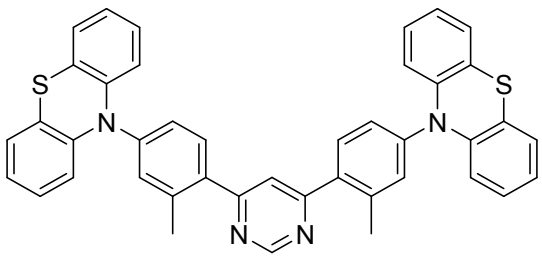

Starting with 4,6-dichloropyrimidine (**1a**) and 2-methyl-4-(10*H*-phenothiazin-10-yl)phenylboronic acid (**2**), compound **PTZ-mPYR** was obtained as a yellow solid (174 mg, 79%), mp 125 °C. ^{1}H NMR (400 MHz, $CDCl_3$) δ (ppm): 9.47 (1H, s, pyrimidine-2-H), 7.75 – 7.80 (3H, m, 2xPh-6-H, pyrimidine-5-H), 7.36 – 7.41 (4H, m, 2xPh-3,5-H); 7.12 (4H, d, *J* = 7.8 Hz, 2x-phenothiazine-4,6-H), 6.88 – 6.99 (8H, m, 2x-phenothiazine-2,3,7,8-H), 6.47 (4H, d, *J* = 7.8 Hz, 2x-phenothiazine-1,9-H), 2.60 (6H, s, 2xCH_3). ^{13}C NMR (100 MHz, $CDCl_3$) δ (ppm): 166.6, 158.5, 143.7, 142.8, 139.2, 136.8, 132.0, 131.6, 127.1, 127.0, 126.9,

123.1, 122.0, 121.0, 117.4, 20,8. HRMS-ESI: m/z calcd. for $[M+H]^+$ ($C_{42}H_{31}N_4S_2$): 655.1984, found: 655.1979.

e) 4,6-Bis(2-methyl-4-(10*H*-phenothiazin-10-yl)phenyl)-2-chloropyrimidine (PTZ-mPYRCl)

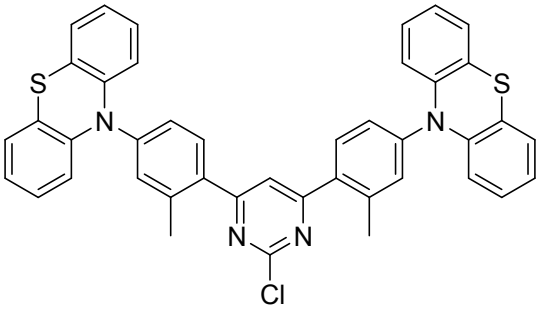

Starting with 2,4,6-trichloropyrimidine (**1b**) and 2-methyl-4-(10*H*-phenothiazin-10-yl)phenylboronic acid (**2**), compound **PTZ-mPYRCl** was obtained as a yellow solid (135 mg, 60%), mp 148-150 °C. ^{1}H NMR (400 MHz, $CDCl_3$) δ (ppm): 7.75 (2H, d, *J* = 8.0 Hz, 2xPh-6-H); 7.65 (1H, s, pyrimidine-5-H); 7.34 – 7.36 (4H, m, 2xPh-3,5-H); 7.15 (4H, d, *J* = 8.0 Hz, 2x-phenothiazine-4,6-H); 6.93 – 7.00 (8H, m, 2x-phenothiazine-2,3,7,8-H); 6.53 (4H, d, *J* = 8.0 Hz, 2x-phenothiazine-1,9-H); 2.60 (6H, s, 2xCH_3). ^{13}C NMR (100 MHz, $CDCl_3$) δ (ppm): 169.4, 161.1, 143.7, 143.4, 139.4, 135.0, 132.0, 130.6, 127.3, 127.0, 126.0, 123.4, 123.0, 119.0, 118.2, 20.9. HRMS-ESI: m/z calcd. for $[M]^+$ ($C_{42}H_{29}ClN_4S_2$): 688.1516, found: 688.1512.

f) 4,6-Bis(4-bromo-2,5-dimethylphenyl)pyrimidine (4)

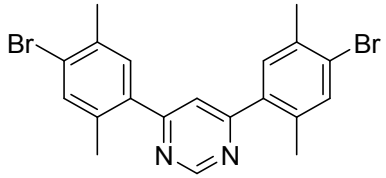

Starting with 4,6-dichloropyrimidine (**1a**) and 4-bromo-2,5-dimethylphenylboronic acid (**3**), compound **4** was obtained as a yellow solid (120 mg, 80%), mp 125-127 °C. ^{1}H NMR (400 MHz, $CDCl_3$) δ (ppm): 9.36 (1H, d, *J* = 4.0 Hz, pyrimidine-2-H); 7.54 (2H, s, 2xPh-3-H); 7.51 (1H, d, *J* = 4 Hz, pyrimidine-5-H); 7.40 (2H, s, 2xPh-6-H); 2.44 (12H, s, 4xCH^3). ^{13}C NMR (100 MHz, $CDCl_3$) δ (ppm): 166.3, 158.5, 136.9, 135.9, 135.2, 134.8, 131.8, 126.4, 120.7, 22.3, 19.8. HRMS-ESI: m/z calcd. for $[M+H]^+$ ($C_{20}H_{19}Br_2N_2$): 444.9910, found: 444.9918.

g) 4,6-Bis(2,5-dimethyl-4-(10*H*-phenothiazin-10-yl)phenyl)pyrimidine (PTZ-2mPYR)

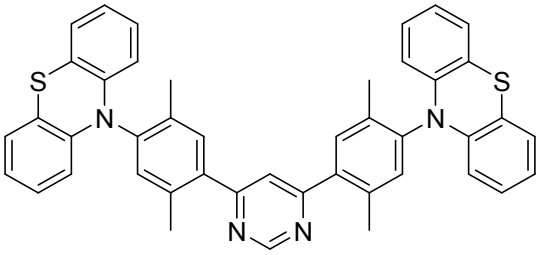

4,6-Bis(4-bromo-2,5-dimethylphenyl)pyrimidine (**4**) (50 mg, 0.11 mmol), $Pd(OAc)_2$ (1.3 mg, 0.0055 mmol, 5 mol %), P(*t*-Bu)$_3$*HBF_4 (3.3 mg, 0.011 mmol, 10 mol %), phenothiazine (47 mg, 0.231 mmol), NaO*t*-Bu

(43 mg, 0.44 mmol, 4 equiv.) and toluene (2 mL) were placed in a screw-cap vial equipped with a magnetic stir bar. The reaction mixture was stirred vigorously at 100 °C for 24 h under argon atmosphere. After completion of the reaction, water (20 mL) was added and the aqueous solution was extracted with chloroform (4×20 mL). The combined extract was dried with anhydrous Na_2SO_4, filtered, and chloroform was removed by distillation under reduced pressure. Residue was purified by column chromatography using chloroform:petroleum ether (1:2) as eluent to give **PTZ-2mPYR** as a light brown solid (56 mg, 73%), mp 238-240 °C. ^{1}H NMR (400 MHz, $CDCl_3$) δ (ppm): 9.48 (1H, s, pyrimidine-2-H); 7.78 (1H, s, pyrimidine-5-H); 7.68 (2H, s, 2xPh-3-H); 7.37 (2H, s, 2xPh-6-H); 6.99 (4H, d, *J* = 8 Hz, 2x-phenothiazine-4,6-H); 6.81 – 6.89 (8H, m, 2x-phenothiazine-2,3,7,8-H); 6.11 (4H, d, *J* = 8 Hz, 2x-phenothiazine-1,9-H); 2.57 (6H, s, 2xCH_3); 2.28 (6H, s, 2xCH_3). ^{13}C NMR (100 MHz, $CDCl_3$) δ (ppm): 166.7, 158.6, 142.5, 140.3, 138.2, 136.8, 136.4, 134.1, 133.6, 127.0, 126.6, 122.4, 121.1, 119.1, 114.9, 20.2, 17.4. HRMS-ESI: m/z calcd. for $[M]^+$ ($C_{44}H_{34}N_4S_2$): 682.2219, found: 682.2210.

^{1}H and ^{13}C NMR spectra of the synthesized compounds

10-(4-Bromo-3-methylphenyl)-10*H*-phenothiazine (I)

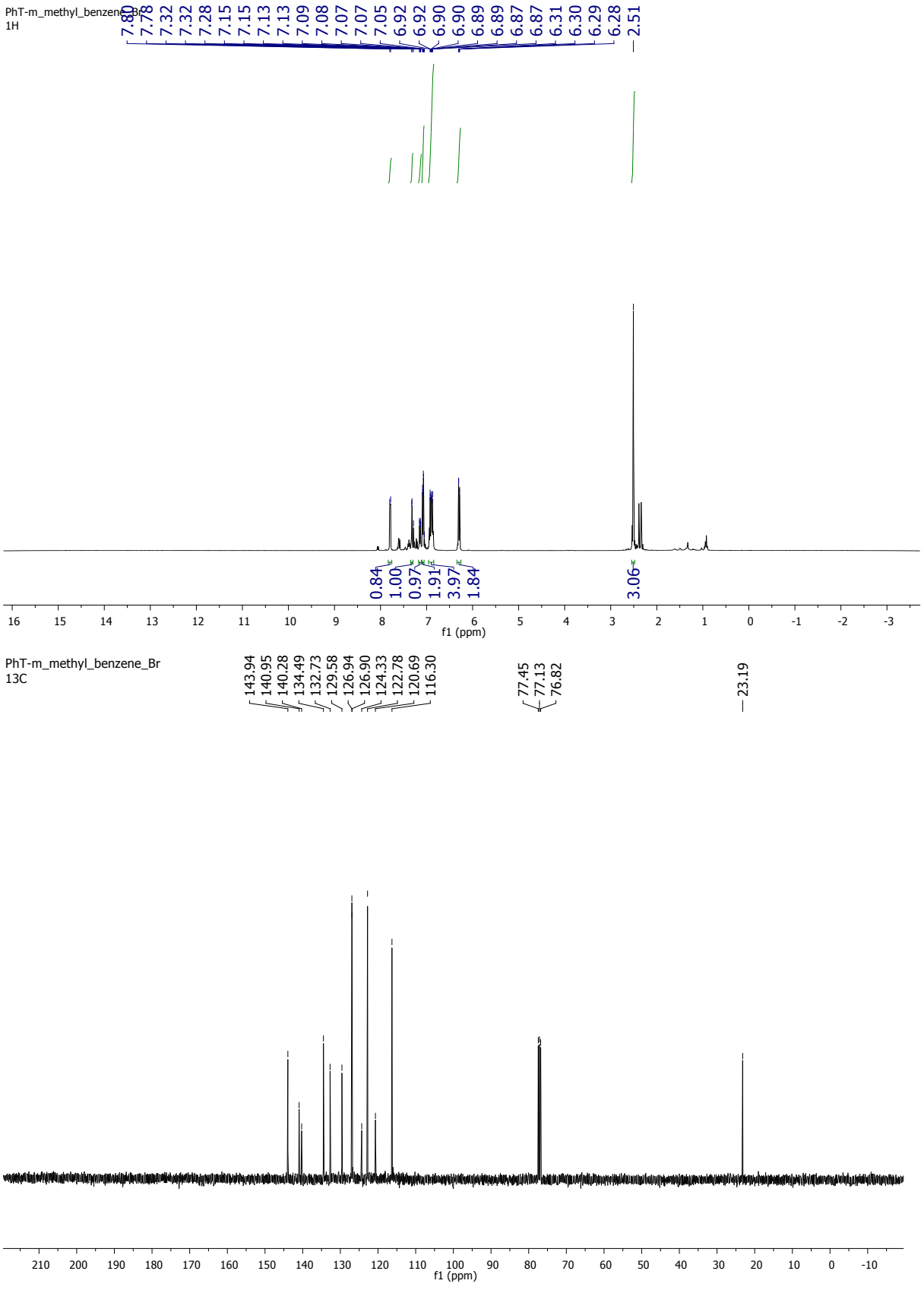

2-Methyl-4-(10*H*-phenothiazin-10-yl)phenylboronic acid (2).

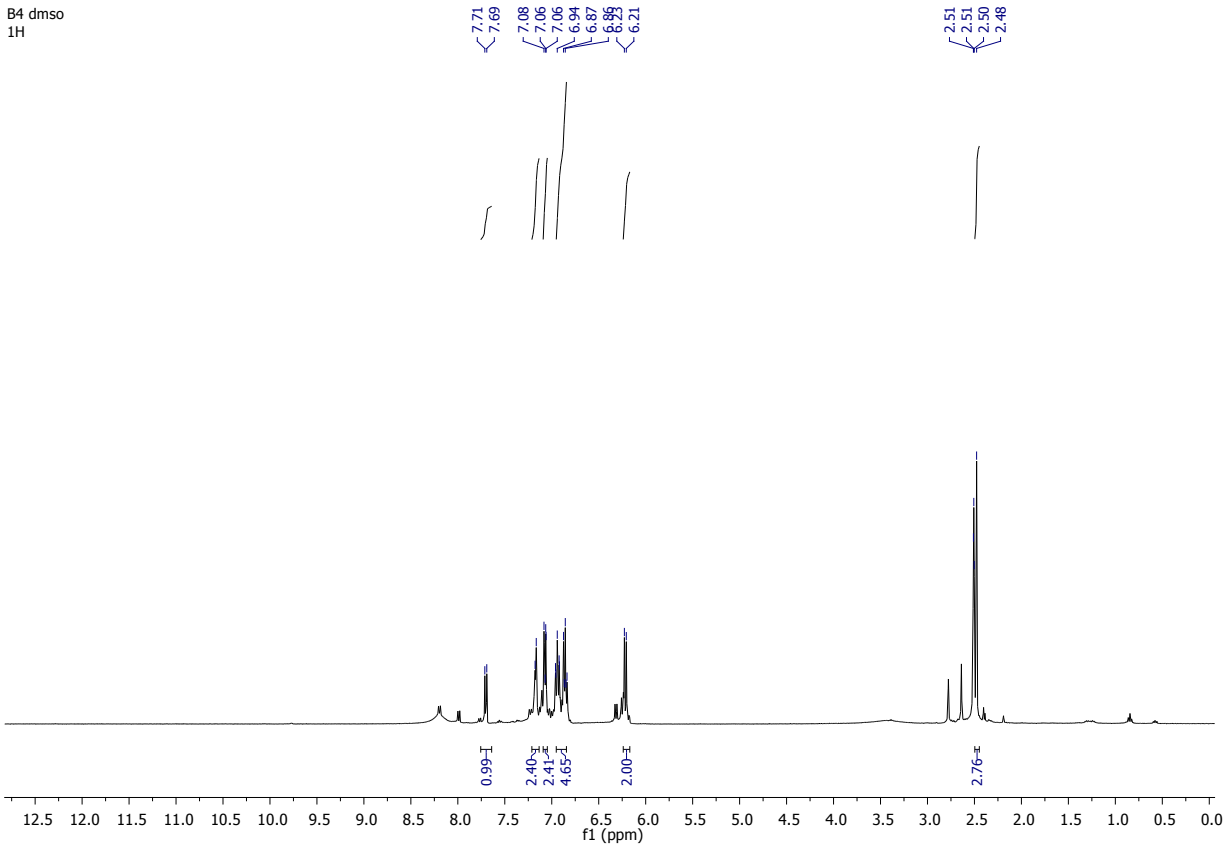

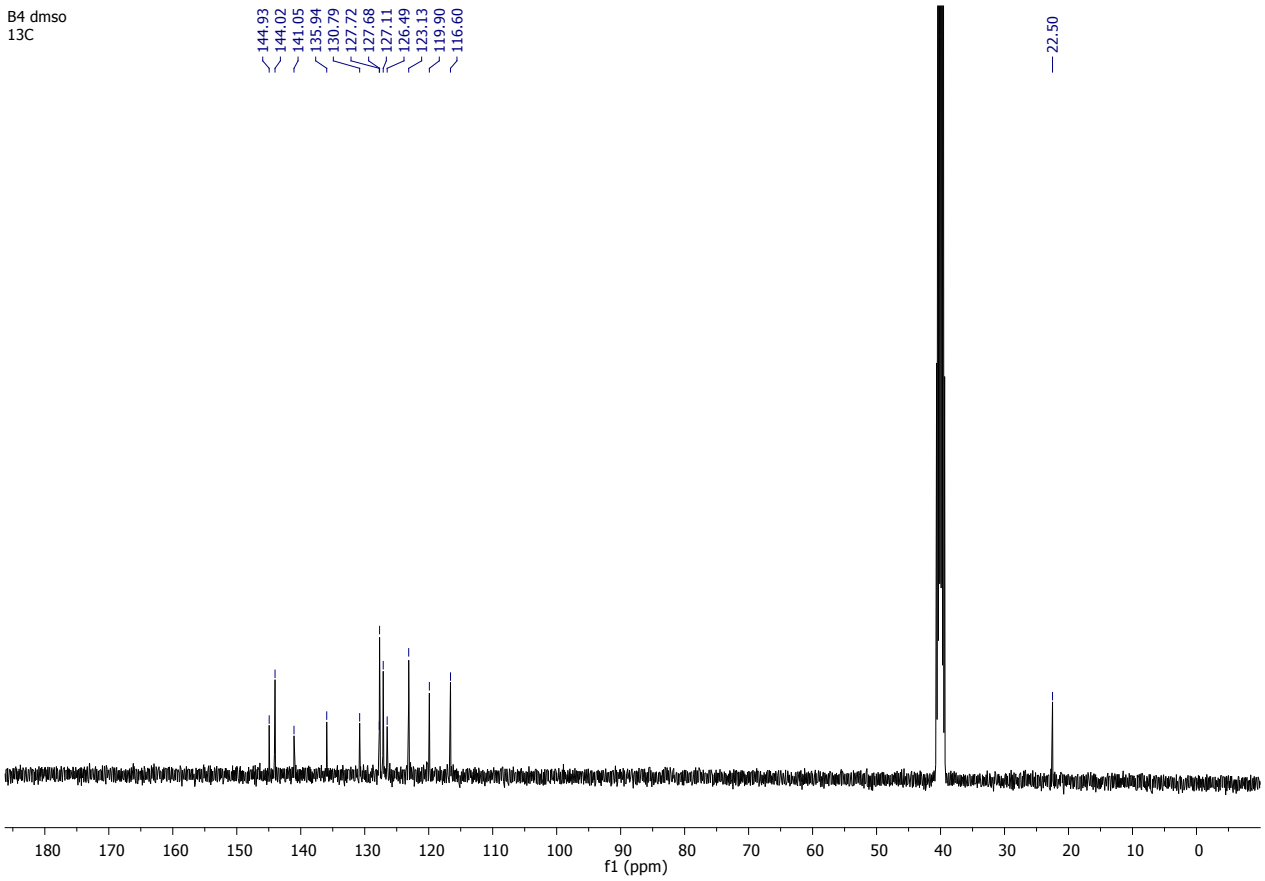

4-bromo-2,5-dimethylphenylboronic acid (3).

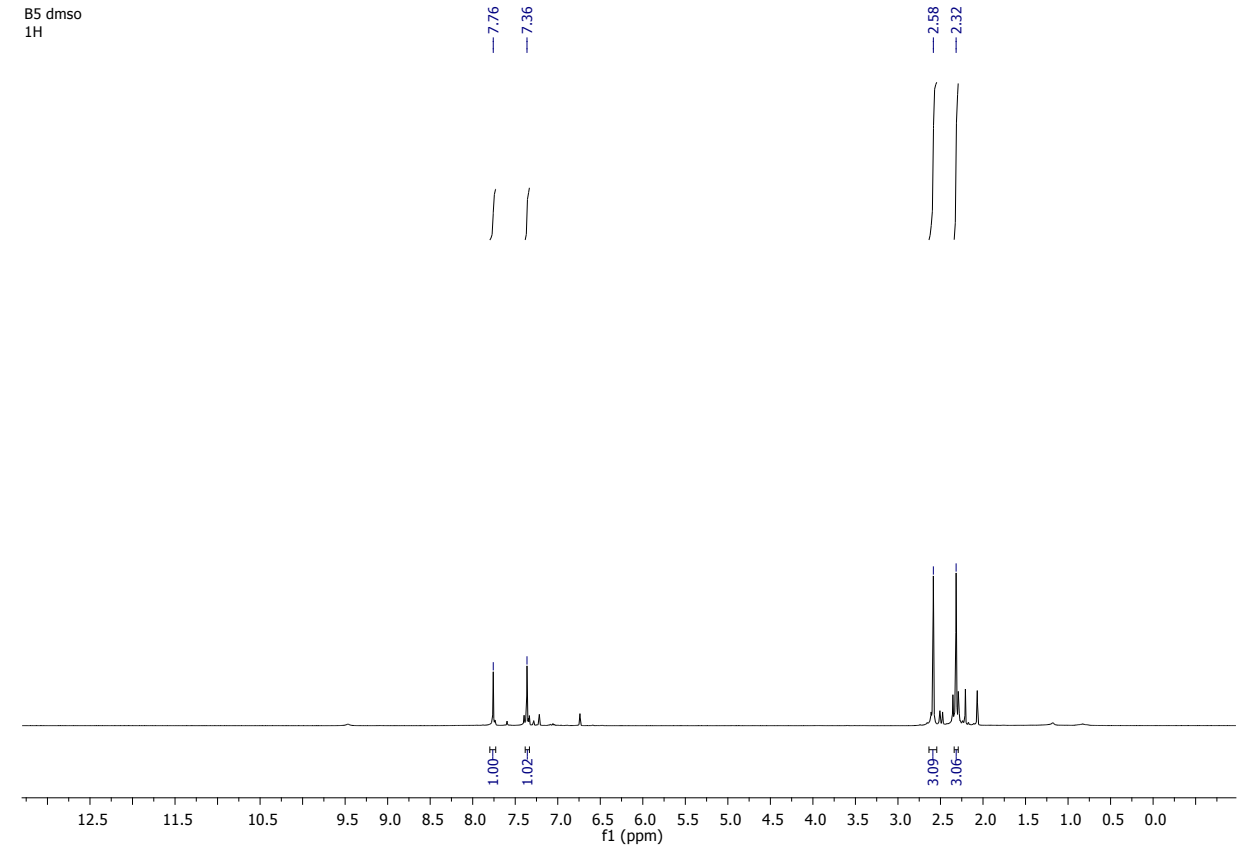

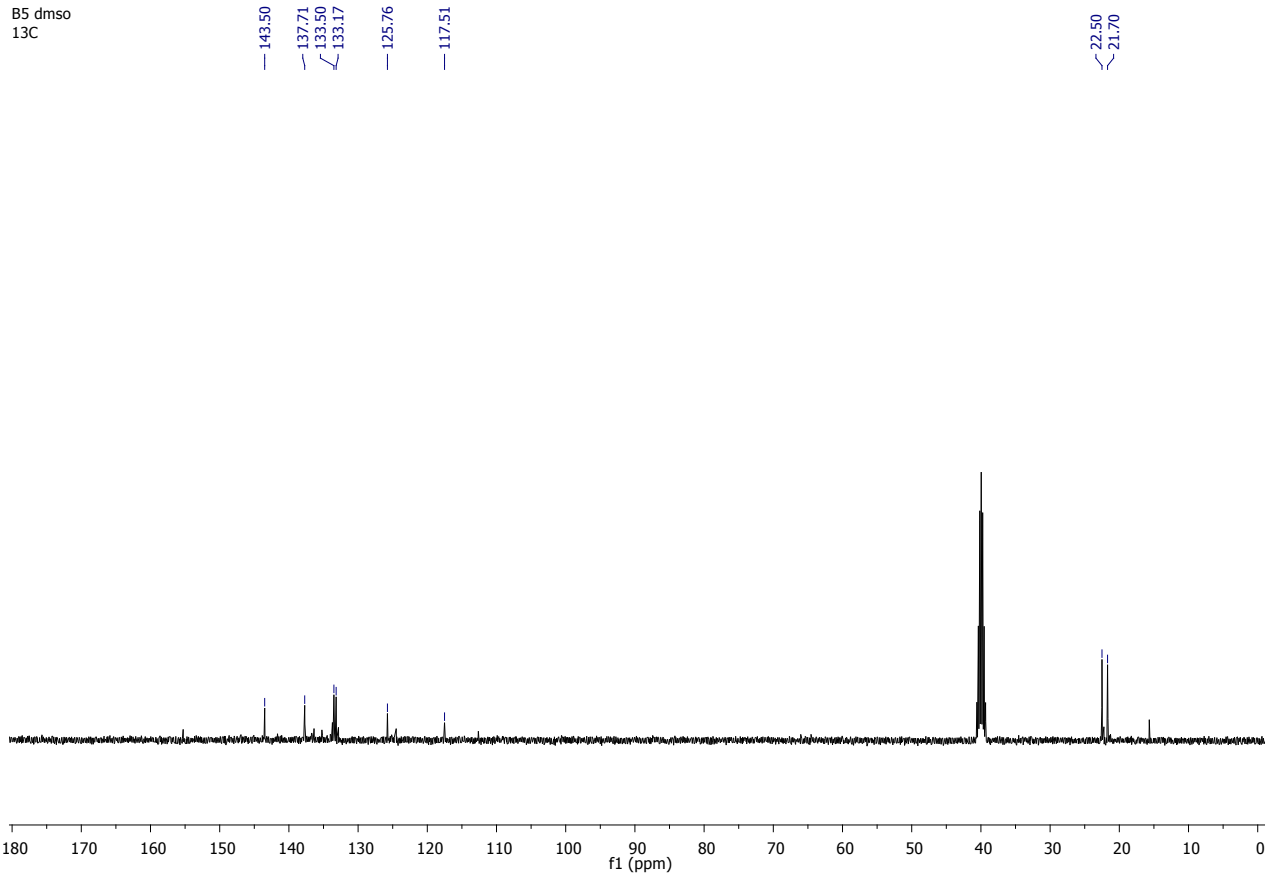

4,6-Bis(4-bromo-2,5-dimethylphenyl)pyrimidine (4).

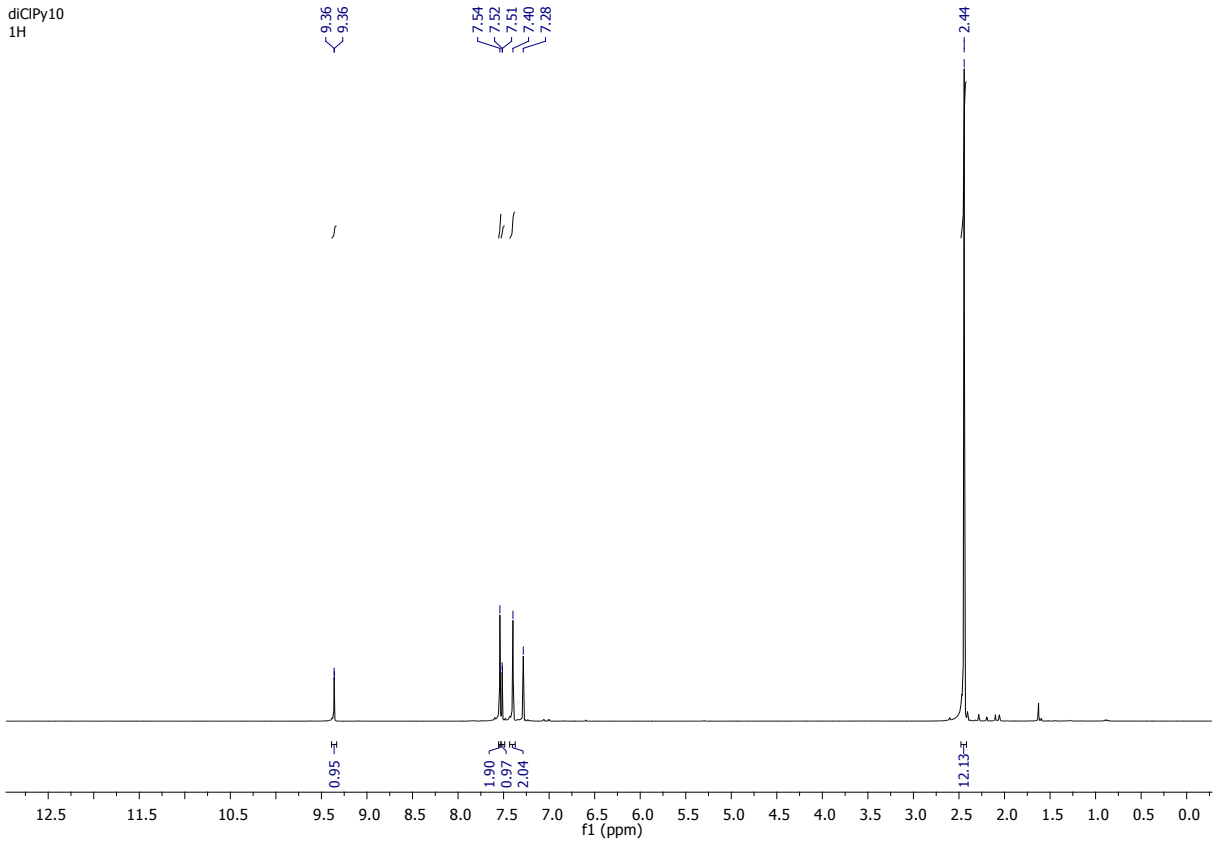

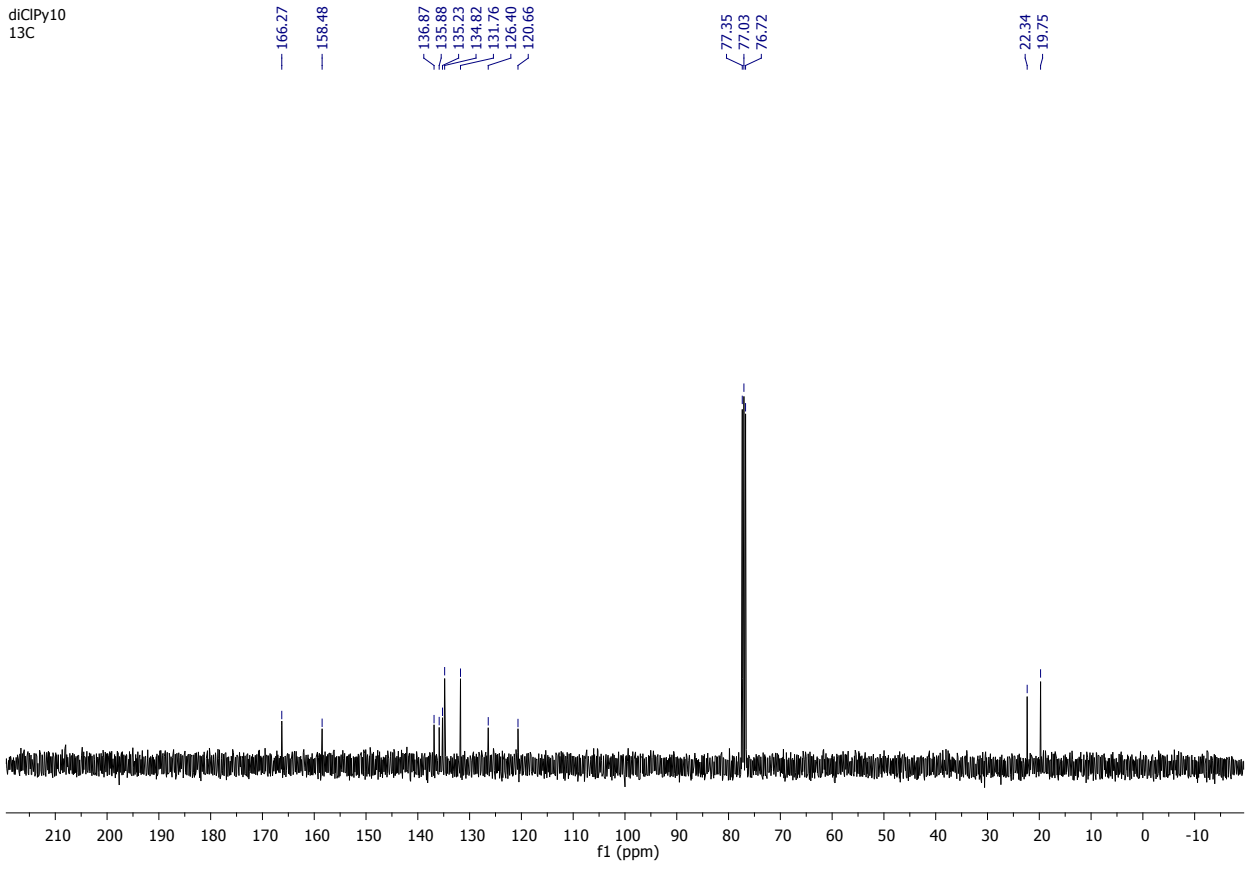

4,6-Bis[2-methyl-4-(10*H*-phenothiazin-10-yl)phenyl]pyrimidine (PTZ-mPYR).

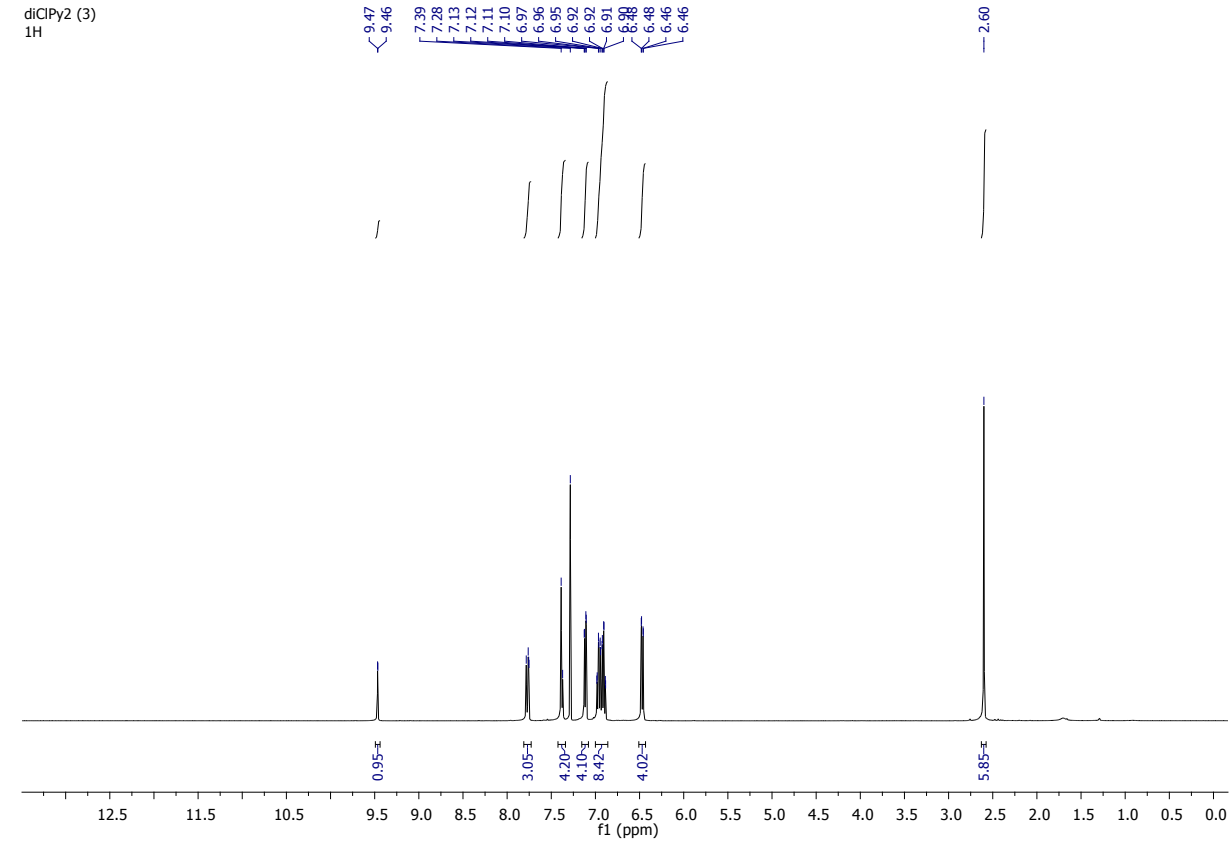

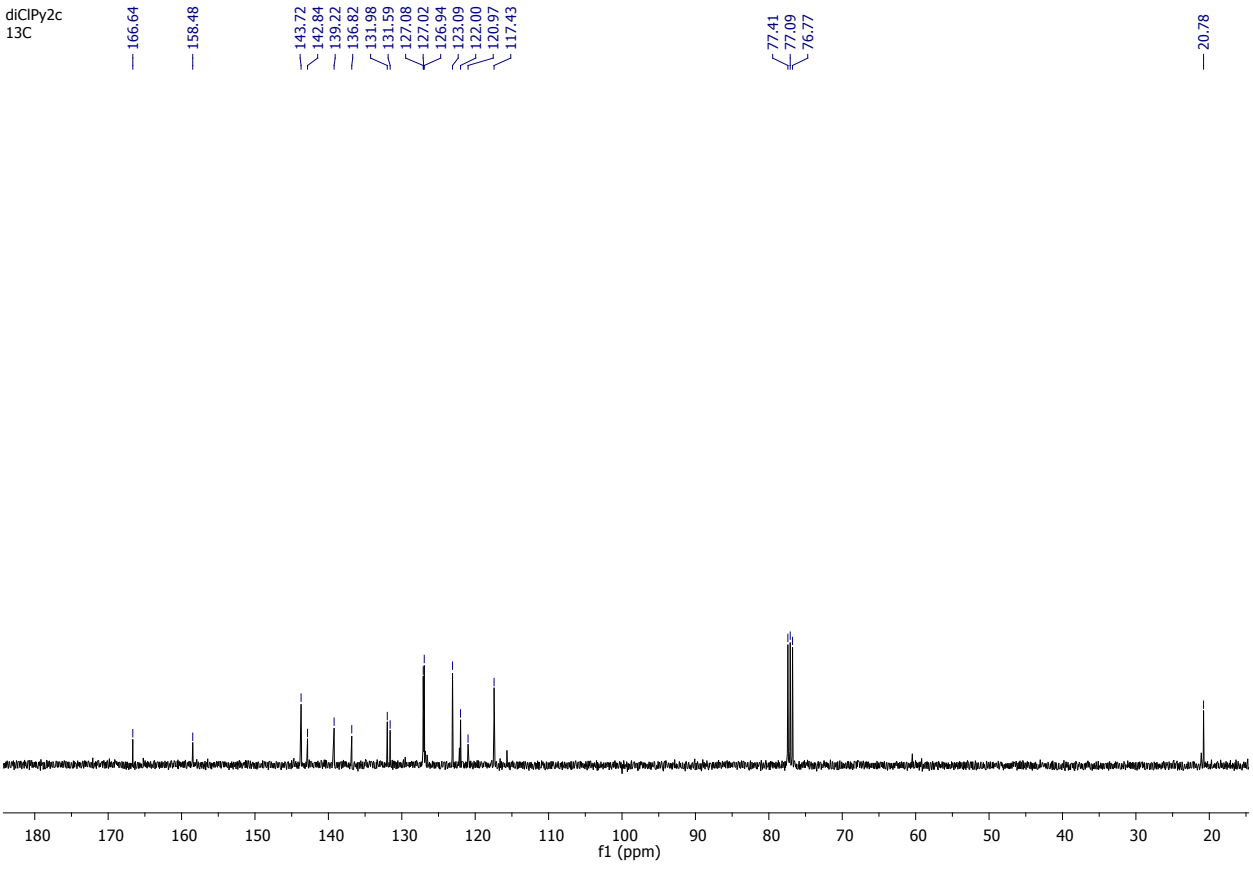

4,6-Bis(2-methyl-4-(10*H*-phenothiazin-10-yl)phenyl)-2-chloropyrimidine (PTZ-mPYRCl).

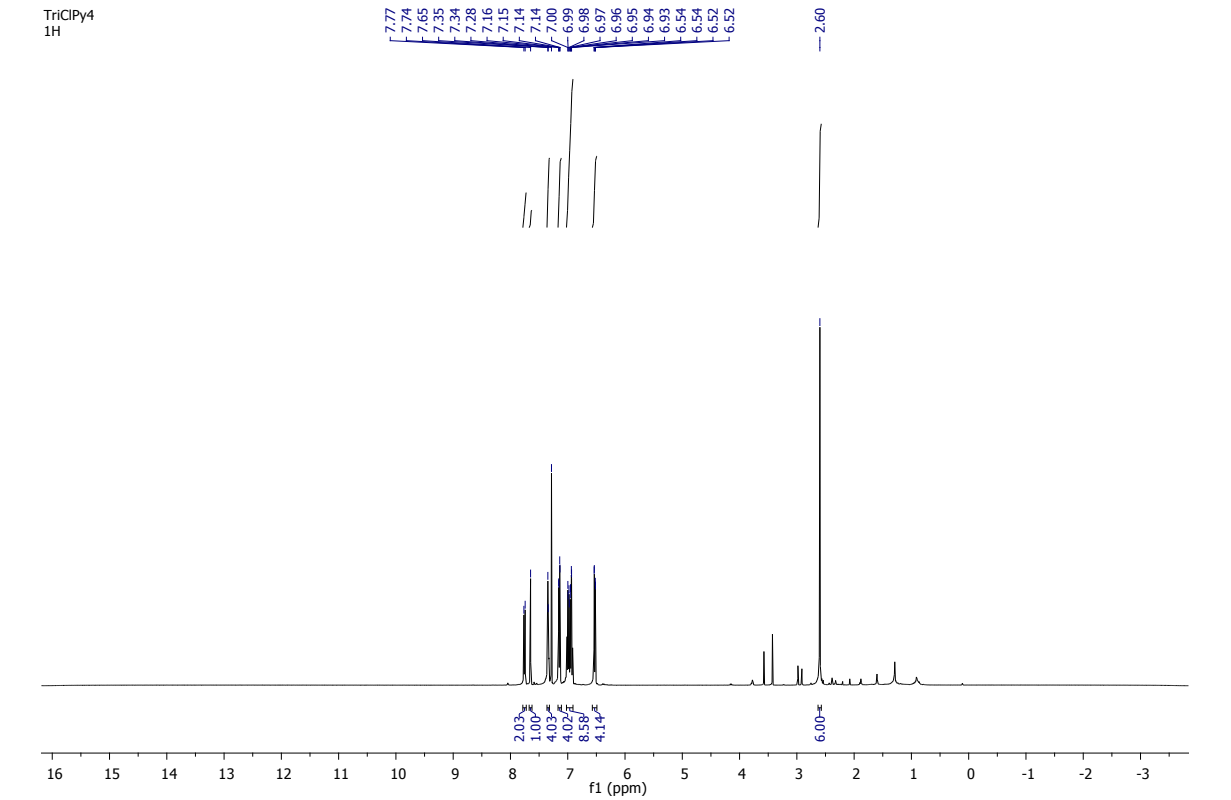

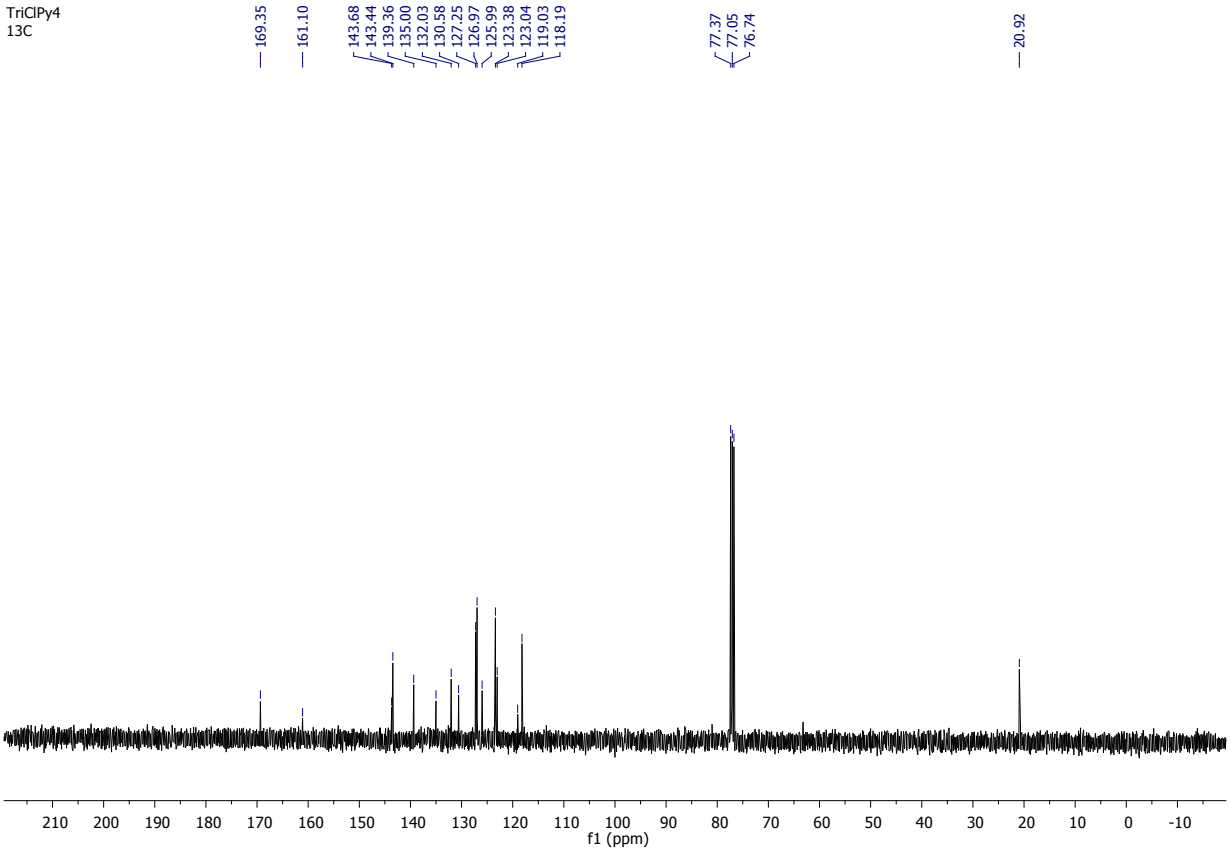

4,6-Bis(2,5-dimethyl-4-(10*H*-phenothiazin-10-yl)phenyl)pyrimidine (PTZ-2mPYR)

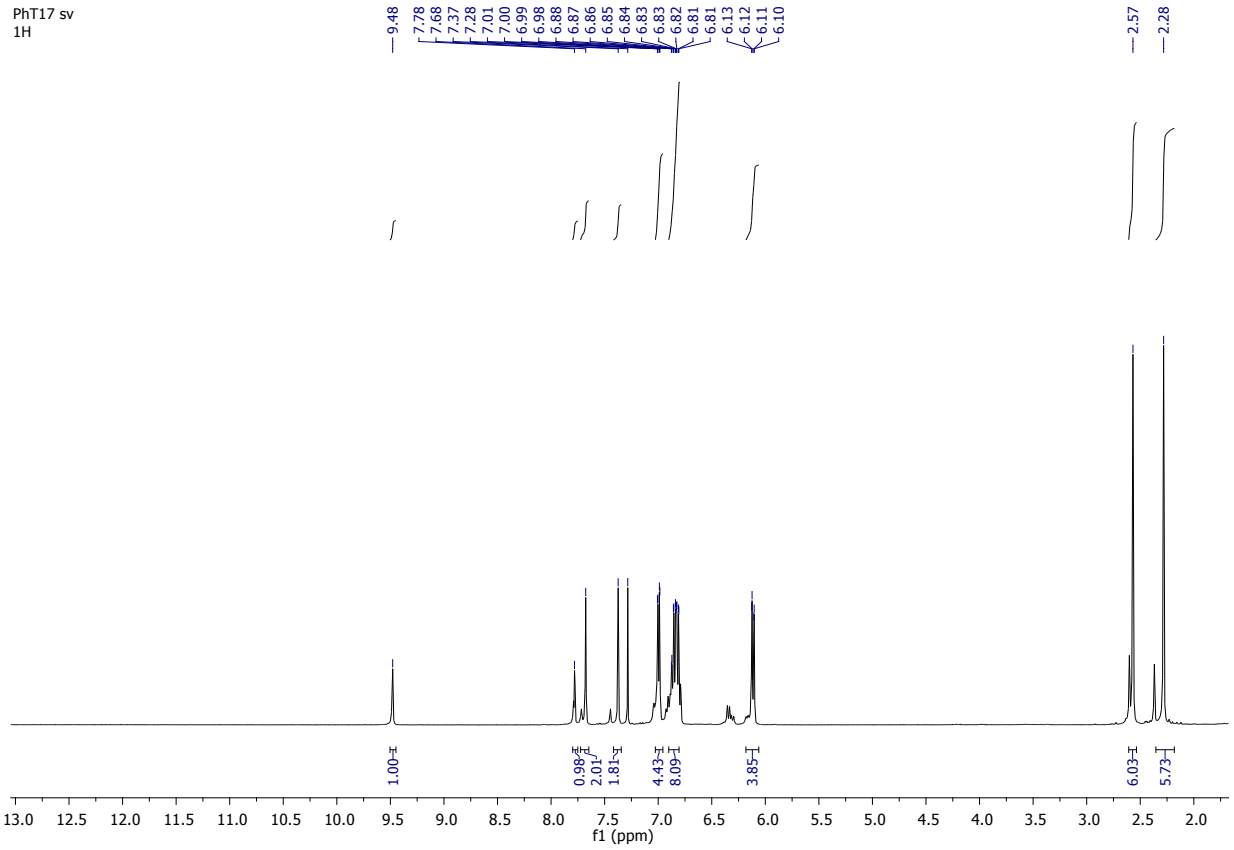

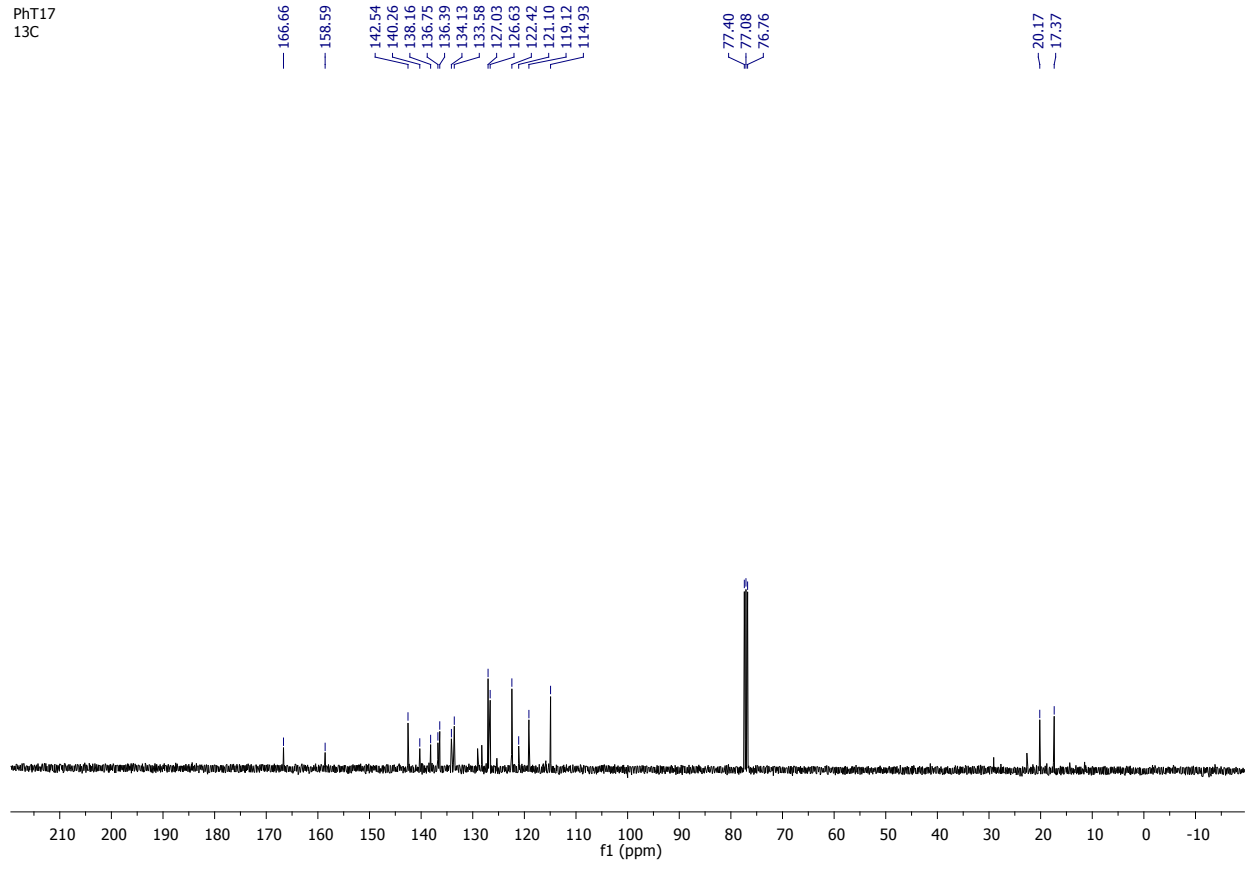

Electrochemical properties

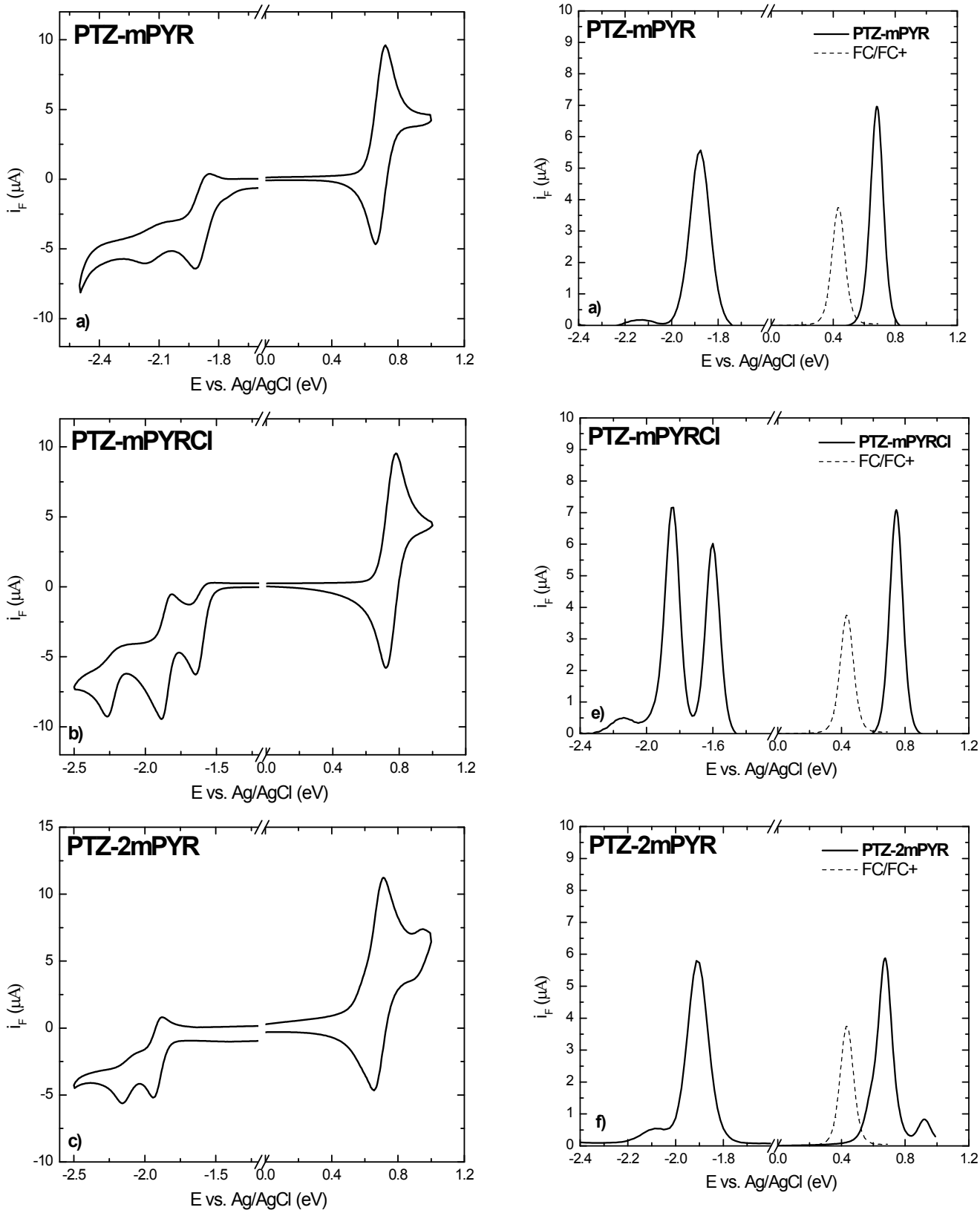

Figure S1. Cyclic (**a**, **b, c**) and differential pulse (**d**, **e, f**) voltammograms of phenothiazine-pyrimidine derivatives: **PTZ-mPYR** (**a, d**), **PTZ-mPYRCl** (**b, e**), **PTZ-2mPYR** (**c, f**) in DMF solution (0.002 M). Supporting electrolyte – tetrabutylammonium perchlorate. Measurements were carried out with glassy carbon working electrode and platinum/titanium auxiliary electrode and values calibrated against Fc/Fc+ couple. Scan rate – 50 mV/s for cyclic voltammetry and 20 mV/s for differential pulse voltammetry.

Table S1. Energies of HOMO and LUMO levels, electrochemical bandgaps of the phenothiazine-pyrimidine compounds. HOMO – LUMO energy levels were estimated by relationship: $E_{HOMO/LUMO} = -(4.8\ eV + E_{OX/RED} - E_{FC/FC+})$

	Cyclic voltammetry			Differential pulse voltammetry		
Comp.	E_{HOMO} (eV) [a]	E_{LUMO} (eV) [b]	E_g el. (eV) [c]	E_{HOMO} (eV) [a]	E_{LUMO} (eV) [b]	E_g el. (eV) [c]
PTZ-mPYR	-5.07	-2.48	2.58	-5.053	-2.493	2.56
PTZ-mPYRCl	-5.12	-2.79	2.34	-5.114	-2.768	2.35
PTZ-2mPYR	-5.05	-2.46	2.59	-4.987	-2.465	2.52

a) HOMO energy levels.

b) LUMO energy levels.

c) Electrochemical bandgaps.

Quantum chemical calculations

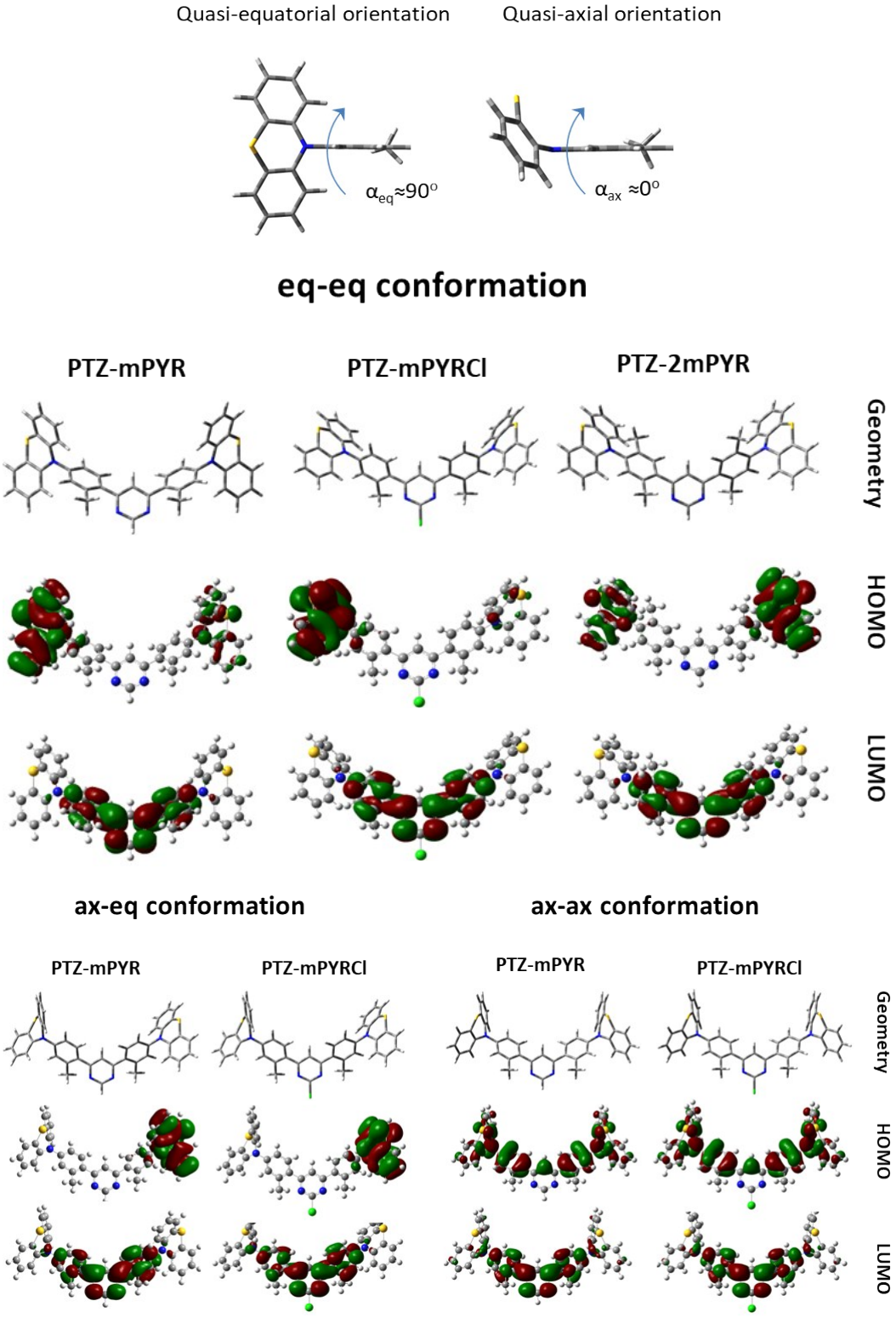

Fig. S2 Optimized geometry of phenothiazine – pyrimidine compounds in quasi-equatorial, quasi-equatorial–quasi-axial and quasi-axial conformations and calculated electron density distribution in HOMO and LUMO.

Table S2 Calculated energies of $S_0 \rightarrow S_1/T_1/T_2$ transitions, oscillator strengths of $S_0 \rightarrow S_1$ transition and energy gaps between the lowest singlet and triplet states of phenothiazine – pyrimidine compounds.

	$f_{S0\rightarrow S1}$ (eV)[a]	$E_{S0\rightarrow S1}$ (eV)[b]	$f_{S0\rightarrow S2}$ (eV)[a]	$E_{S0\rightarrow S2}$ (eV)[b]	$E_{S0\rightarrow T1}$ (eV)[b]	$E_{S0\rightarrow T2}$ (eV)[b]	ΔE_{S0T1} (meV)[c]
quasi-equatorial conformation							
PTZ-mPYR	0.0009	2.7744	0.0001	2.7745	2.7603	2.7605	14
PTZ-mPYRCl	0.0005	2.5629	0.0003	2.5630	2.5548	2.5549	8
PTZ-2mPYR	0.0001	2.8111	0.0004	2.8111	2.7908	2.7908	20
quasi-equatorial – quasi axial conformation							
PTZ-mPYR	0.0003	2.9791	0.5306	3.3609	2.8414	2.9350	138
PTZ-mPYRCl	0.0003	2.7756	0.5712	3.2068	2.7203	2.7615	55.3
PTZ-2mPYR	-	-	-	-	-	-	-
quasi axial conformation							
PTZ-mPYR	1.0180	3.3995	0.1971	3.6279	2.8957	2.9429	457
PTZ-mPYRCl	1.0147	3.2337	0.2032	3.4821	2.8078	2.8245	426
PTZ-2mPYR	-	-	-	-	-	-	-

[a] Oscillator strengths of $S_0 \rightarrow S_1$ and $S_0 \rightarrow S_2$ transitions.

[b] Energies of $S_0 \rightarrow S_1$, $S_0 \rightarrow S_2$, $S_0 \rightarrow T_1$ and $S_0 \rightarrow T_2$ transitions.

[c] Energy difference between T_1 and S_0 energy levels.

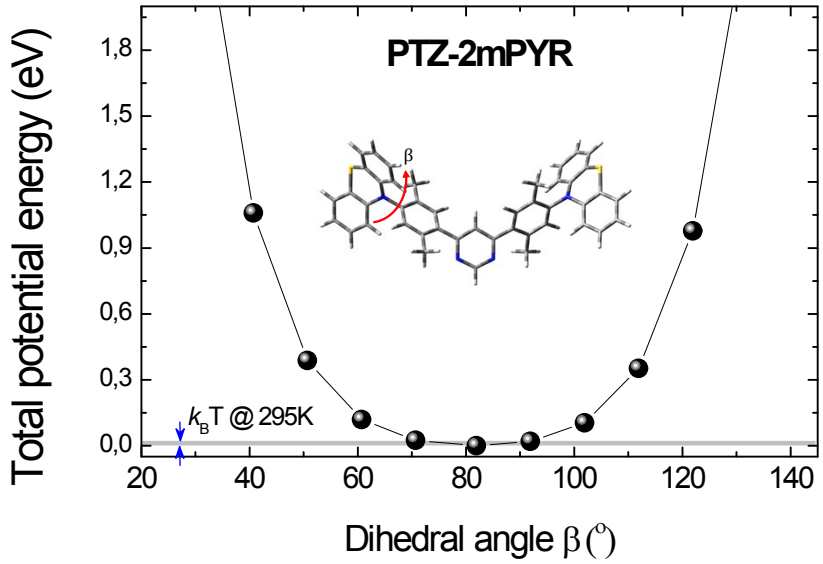

Fig. S3 Potential energy scan for compound **PTZ-2mPYR.** B3LYP/6-31G(d) basis set was used for simulation. The potential energy of the lowest-energy conformer state was set as 0. Left dihedral angle was varied in the range of -10 – 190° without structure optimization. The right PTZ unit was kept at fixed orientation. Ground state energy for "freezed" structures was calculated using single point routine.

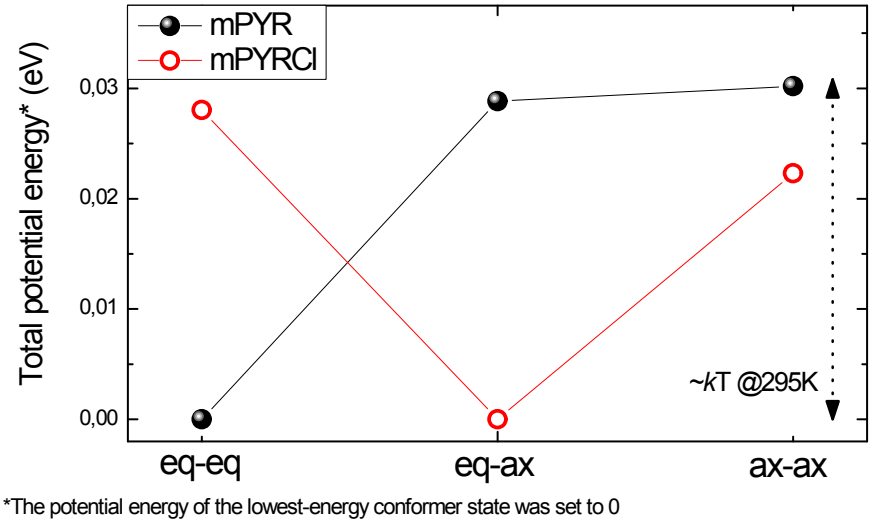

Fig. S4 Total potential molecular energies of ground state optimized conformers of compounds **PTZ-mPYR** (black figures) and **PTZ-mPYRCl** (red figures).

Table S3 Total potential energies of diferent conformers for compounds **PTZ-mPYR** and **PTZ-mPYRCl**.

	PTZ-mPYR	**PTZ-mPYRCl**
Conformer	TPE (meV)	TPE (meV)
eq-eq	0	28
eq-ax	29	0
ax-ax	30	23

TPE – total potential energy

Extended fluorescence properties

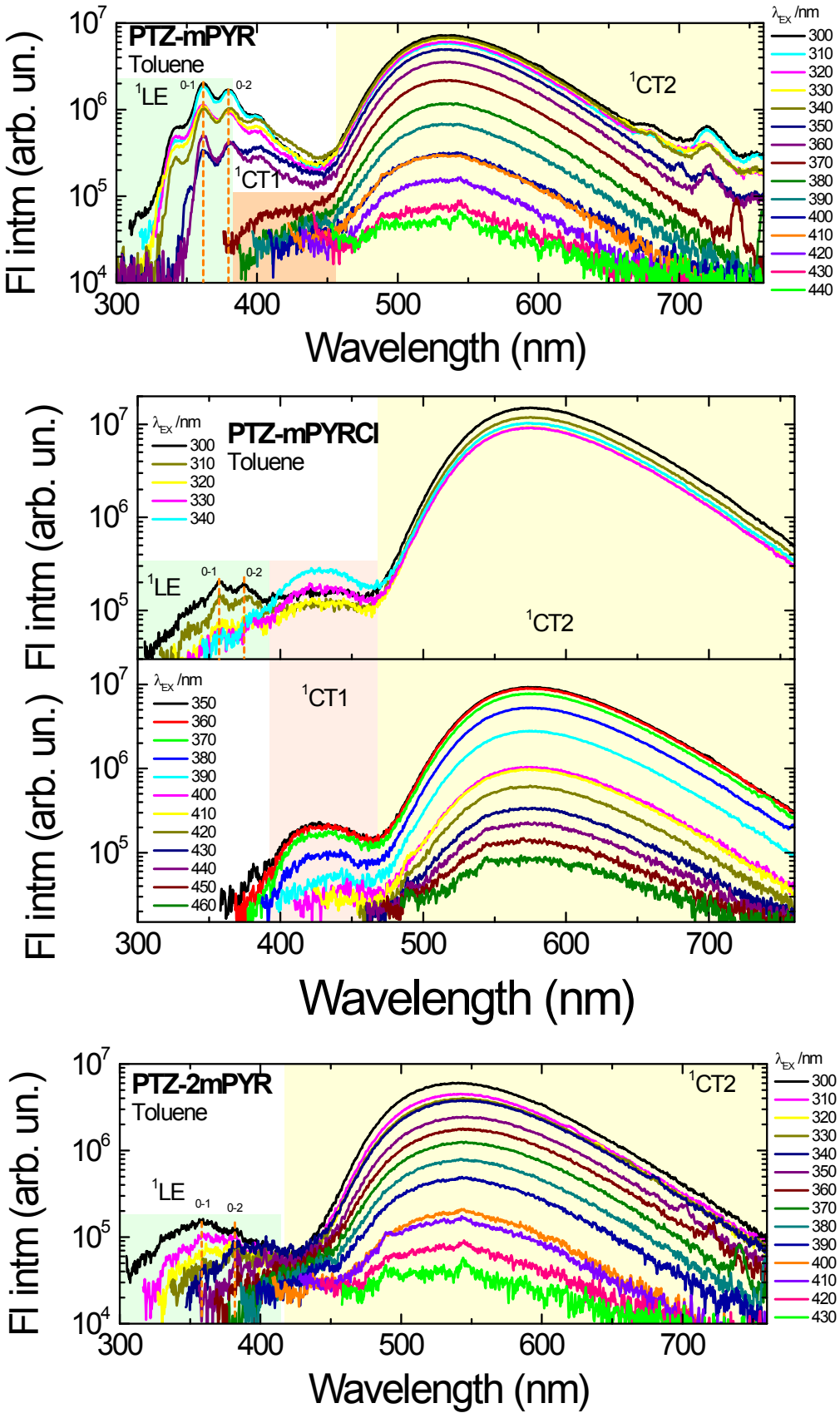

Fig. S5 Fluorescence spectra of phenothiazine – pyrimidine compounds in toluene obtained after photoexcitation with different wavelength light (λ_{ex}).

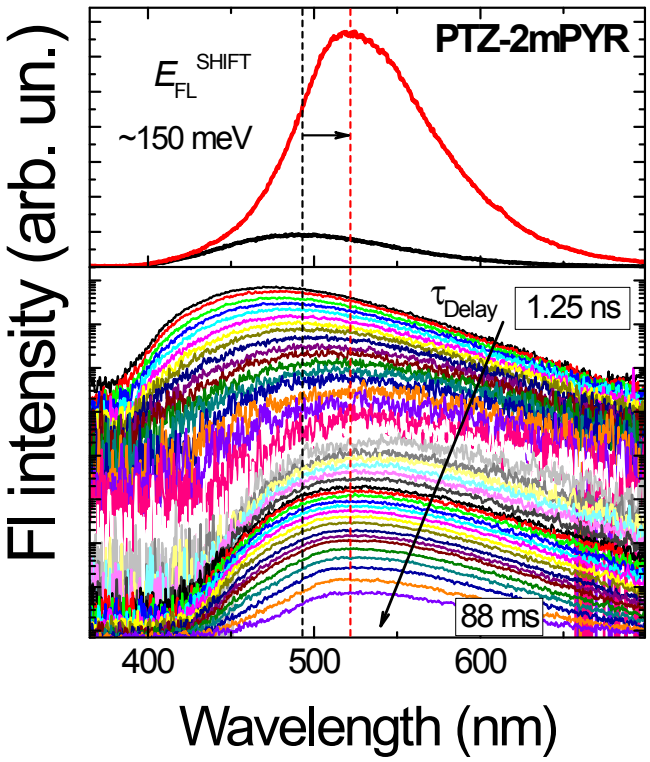

Fig. S6 Time-integrated fluorescence spectra of 1wt% PMMA film of **PTZ-2mPYR** in oxygen-sufficient (O2+, black lines) and oxygen-deficient (O2-, red line) surroundings (upper picture). Time-resolved fluorescence spectra of 1wt% PMMA film of **PTZ-2mPYR** in oxygen-deficient surrounding (lower picture). Numbers denote initial and final delay time.

Analysis of DF nature

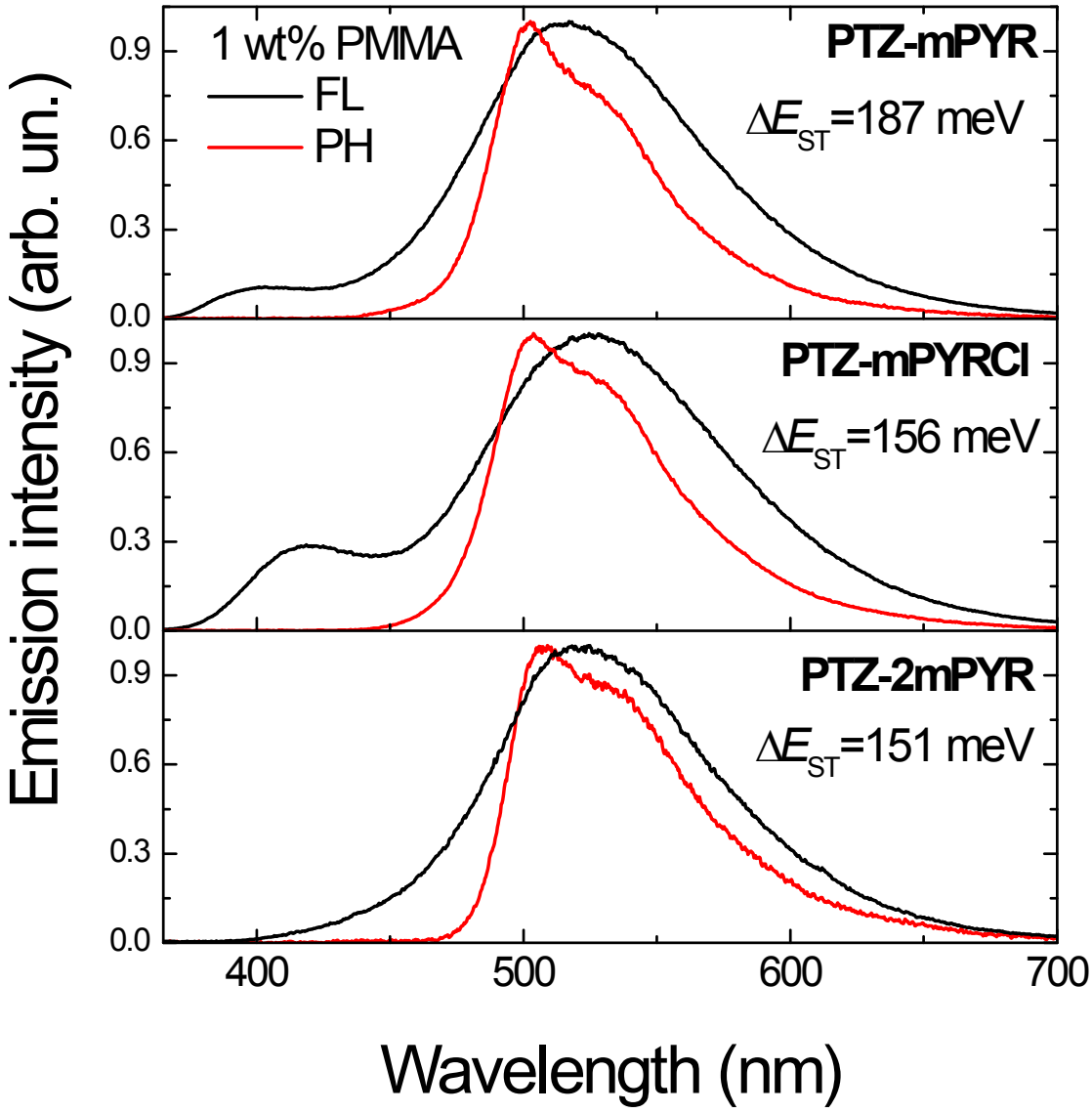

Fig. S7 Room temperature fluorescence (black lines) and phosphorescence (red lines) spectra at 50K of phenothiazine – pyrimidine compounds in 1 wt% PMMA films. Energy gaps between the lowest singlet ($^1CT_{QE}$) and triplet states, estimated from the spectral on-sets, are also shown (ΔE_{ST}). Phosphorescence spectrum can be attributed to phenothiazine donor group[4].

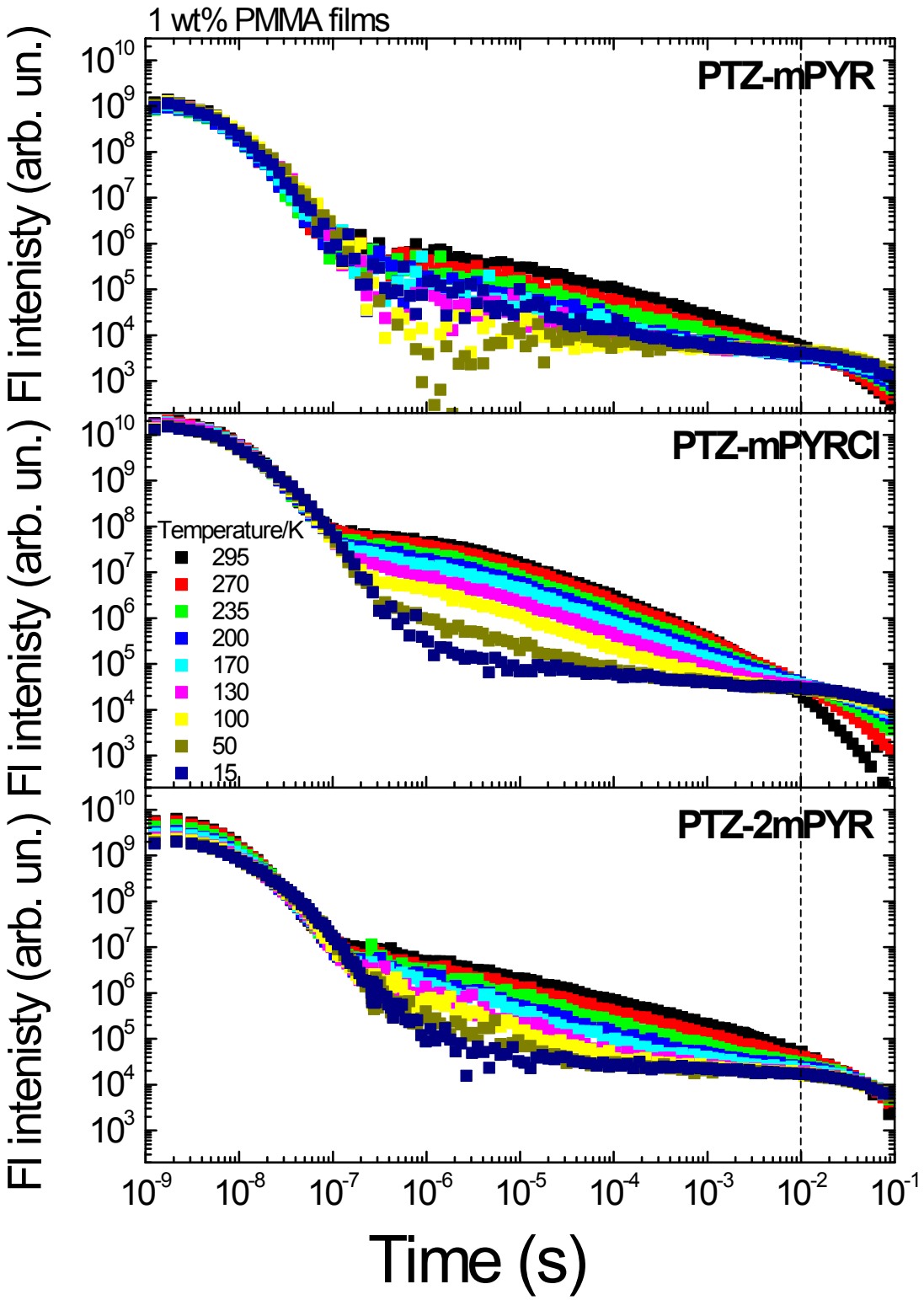

Fig. S8 Fluorescence decay transients of 1 wt% PMMA films of phenothiazine – pyrimidine compounds at different temperatures in oxygen-free ambient at $^1CT_{QE}$ peak.

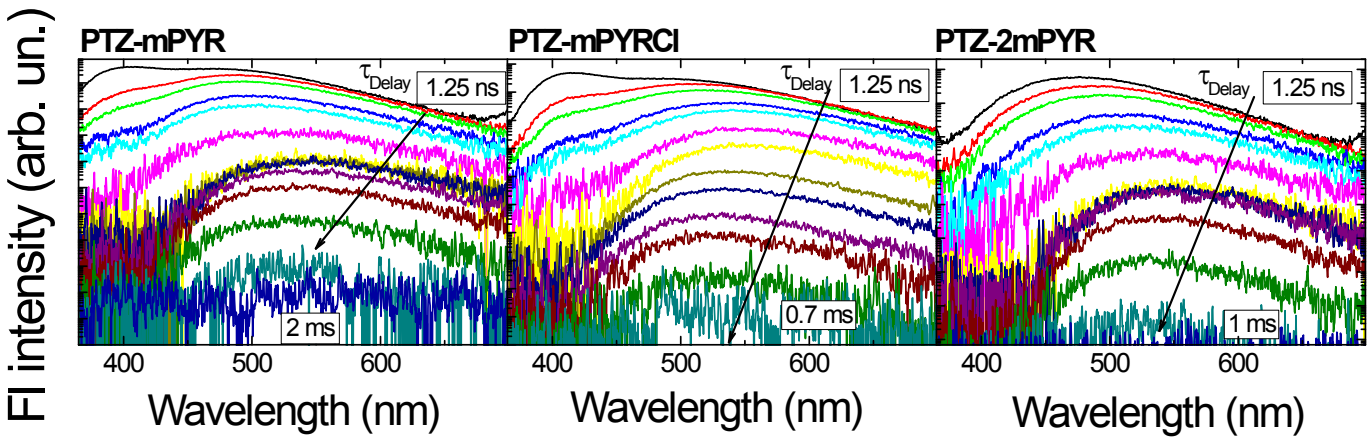

Fig. S9 Time-resolved fluorescence spectra of 1wt% PMMA films of **PTZ-mPYR**, **PTZ-mPYRCl** and **PTZ-2mPYR** in oxygen-saturated ambient. Numbers denotes the initial and latest delay times.

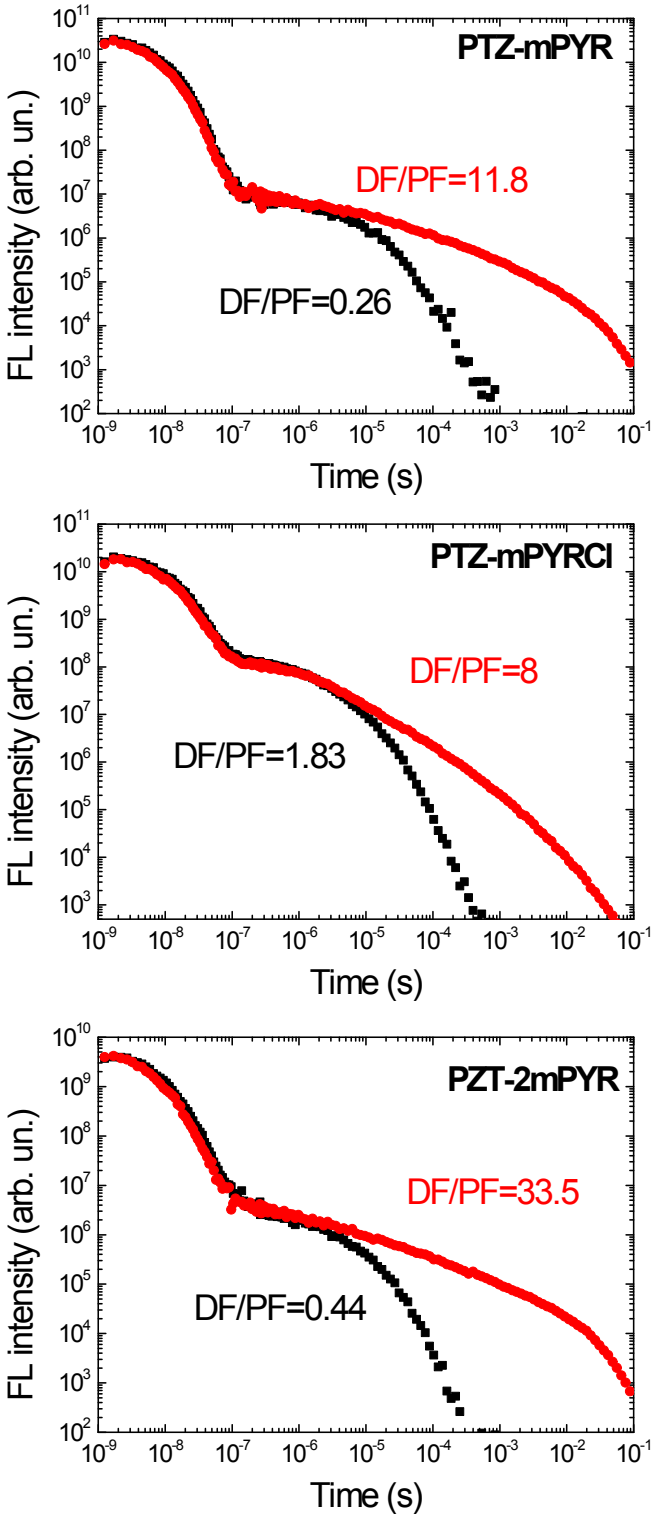

Fig. S10 $^1CT_{QE}$ fluorescence decay transients of 1 wt% PMMA films of phenothiazine – pyrimidine compounds in oxygen-saturated (0_2+, black figures) and oxygen-free (0_2-,red figures) conditions. DF/PF ratio denotes the ratio between the integrated intensities of delayed and prompt fluorescence.

Evaluation of the rISC rate

rISC rate (k_{rISC}) for TADF compounds with low DF/PF ratio (below 3 or 4) is determined according to equation 1[5]:

$$k_{rISC} = \frac{k_{TADF}}{\Phi_{ISC}}\left(\frac{\Phi_{TADF}}{\Phi_{PF}}\right) \quad (1).$$

In this case reverse intersystem crossing yield (Φ_{rISC}) cannot be assumed to be equal to ≈1, thus Φ_{ISC} should be determined according to equation 2[6]:

$$\tau_{TADF} = \tau_{PH}^{0} - \left(\frac{1}{\Phi_{ISC}} - 1\right)\tau_{PH}^{0}\frac{\Phi_{TADF}}{\Phi_{PF}} \quad (2).$$

τ_{TADF}, Φ_{TADF}/Φ_{PF} ratio and τ_{PH}^{0} (phosphorescence lifetime when rISC is non-operative, see Fig. S7) are known, thus Φ_{ISC} can be easily calculated. Intersystem crossing rate (k_{ISC}) then can be obtained from equation 3:

$$k_{ISC} = \frac{\Phi_{ISC}}{\tau_{PF}} \quad (3).$$

The estimated Φ_{ISC}, k_{ISC} and k_{rISC} values are shown in Table S3. Although TADF decay rate in solid state could not be estimated, it should not strongly differ. According to the equation 1, k_{rISC} depends on the product of k_{TADF} and DF/PF ratio. Since the both parameters depend on the conformational disorder, probably even at the same extent, its product is should to be similar to that in solutions. Another parameter, which should directly perturb the k_{rISC} is Φ_{ISC} (equation 2), where the impact of conformational disorder cannot be neglected in the same manner as in case of $k_{TADF}\left(\frac{\Phi_{TADF}}{\Phi_{PF}}\right)$. However, it is clear, that **PTZ-mPYRCl** has the most rapid TADF decay, thus probably and k_{rISC}.

Table S4 PF and DF parameters for compounds **PTZ-mPYR**, **PTZ-mPYRCl** and **PTZ-2mPYR** in toluene.

	k_{PF} (x 10^7 s^{-1})[a]	k_{TADF} (x 10^4 s^{-1})[b]	Φ_{DF}/Φ_{PF}[c]	τ_{PH}^{0} (ms)[d]	Φ_{ISC}[e]	k_{rISC} (x 10^5 s^{-1})[f]	k_{ISC} (x 10^6 s^{-1})[g]
PTZ-mPYR	10.0	9.09	0.3	40	0.23	1.18	27.2
PTZ-mPYRCl	4.39	90.9	1.2	90	0.55	20	35.7
PTZ-2mPYR	9.09	16.7	0.03	50	0.03	1.72	3.2

[a] Prompt fluorescence decay rate.
[b] TADF decay rate.
[c] Intensity ratio of the delayed and prompt fluorescence.
[d] Phosphorescence lifetime.
[e] Intersystem crossing yield.
[f] Reverse intersystem crossing rate.
[g] Intersystem crossing rate.

References

1 C. Rothe and A. Monkman, *Phys. Rev. B*, 2003, **68**, 1–11.

2 Gaussian 09, Revision C.01, M. J. Frisch, G. W. Trucks, H. B. Schlegel, G. E. Scuseria, M. A. Robb, J. R. Cheeseman, G. Scalmani, V. Barone, B. Mennucci, G. A. Petersson, H. Nakatsuji, M. Caricato, X. Li, H. P. Hratchian, A. F. Izmaylov, J. Bloino, G. Zheng, J. L. Sonnenberg, M. Hada, M. Ehara, K. Toyota, R. Fukuda, J. Hasegawa, M. Ishida, T. Nakajima, Y. Honda, O. Kitao, H. Nakai, T. Vreven, J. A. Montgomery, Jr., J. E. Peralta, F. Ogliaro, M. Bearpark, J. J. Heyd, E. Brothers, K. N. Kudin, V. N. Staroverov, T. Keith, R. Kobayashi, J. Normand, K. Raghavachari, A. Rendell, J. C. Burant, S. S. Iyengar, J. Tomasi, M. Cossi, N. Rega, J. M. Millam, M. Klene, J. E. Knox, J. B. Cross, V. Bakken, C. Adamo, J. Jaramillo, R. Gomperts, R. E. Stratmann, O. Yazyev, A. J. Austin, R. Cammi, C. Pomelli, J. W. Ochterski, R. L. Martin, K. Morokuma, V. G. Zakrzewski, G. A. Voth, P. Salvador, J. J. Dannenberg, S. Dapprich, A. D. Daniels, O. Farkas, J. B. Foresman, J. V. Ortiz, J. Cioslowski, and D. J. Fox, Gaussian, Inc., Wallingford CT, 2010.

3 T. Faury, F. Dumur, S. Clair, M. Abel, L. Porte and D. Gigmes, *CrystEngComm*, 2013, **15**, 2067.

4 P. L. dos Santos, J. S. Ward, A. S. Batsanov, M. R. Bryce and A. P. Monkman, *J. Phys. Chem. C*, 2017, **121**, 16462–16469.

5 F. B. Dias, T. J. Penfold and A. P. Monkman, *Methods Appl. Fluoresc.*, 2017, **5**, 012001.

6 C. Baleizão and M. N. Berberan-Santos, *ChemPhysChem*, 2011, **12**, 1247–1250.